Journal of The Electrochemical Society, **161** (3) A410-A415 (2014)
0013-4651/2014/161(3)/A410/6/$31.00 © The Electrochemical Society

A Magnesium-Activated Carbon Hybrid Capacitor

Hyun Deog Yoo,[a] Ivgeni Shterenberg,[a] Yosef Gofer,[a] Robert E. Doe,[b,*] Chris C. Fischer,[b] Gerd Ceder,[b] and Doron Aurbach[a,,z]**

[a]*Department of Chemistry and Bar-Ilan Institute of Nanotechnology and Advanced Materials, Bar-Ilan University, Ramat-Gan, Israel*
[b]*Pellion Technologies, Cambridge, Massachusetts 02138, USA*

Prototype cells of hybrid capacitor were developed, comprising activated carbon (AC) cloth and magnesium (Mg) foil as the positive and negative electrodes, respectively. The electrolyte solution included ether solvent (THF) and a magnesium organo-halo-aluminate complex 0.25 M $Mg_2Cl_3^+$-$Ph_2AlCl_2^-$. In this solution Mg can be deposited/dissolved reversibly for thousands of cycles with high reversibility (100% cycling efficiency). The main barrier for integrating porous AC electrodes with this electrolyte solution was the saturation of the pores with the large ions in the AC prior to reaching the potential limit. This is due to the existence of bulky Mg and Al based ionic complexes consisting Cl, alkyl or aryl (R), and THF ligands. This problem was resolved by adding 0.5 M of lithium chloride (LiCl), thus introducing smaller ionic species to the solution. This Mg hybrid capacitor system demonstrated a stable cycle performance for many thousands of cycles with a specific capacitance of 90 F g^{-1} for the AC positive electrodes along a potential range of 2.4 V.
 [DOI: 10.1149/2.082403jes]

Manuscript submitted November 22, 2013; revised manuscript received December 26, 2013. Published January 9, 2014.

Hybrid capacitors aim at possessing the most important characteristics of super-capacitors, namely high power capabilities and prolonged cycle-life, while having higher specific energy density than that of symmetric super-capacitors, which both electrodes involve only electrostatic interactions. Usually this is realized by assembling an asymmetric cell with an electric double-layer capacitor (EDLC) electrode and a red-ox battery electrode. Ideally, the specific capacitance of a battery electrode (C_{BATT}) can be regarded as semi-infinite. Therefore, the full-cell specific capacitance (C_{tot}) of a hybrid capacitor is dominated by the EDLC electrode. Usually EDLC electrodes are based on high surface area activated carbons (AC) and therefore, the EDLC electrode's capacitance can be approximated to the specific capacitance of the activated carbon (C_{AC}) from which it is made. Consequently, the specific capacitance of hybrid, asymmetric super-capacitor, C_{tot}, is close to that of the activated carbon, C_{AC}.

The relevant formula is: $1/(m_{tot}C_{tot}) = 1/(m_{AC}C_{AC}) + 1/(m_{BATT}C_{BATT})$, where m_x is the mass of component x.

On the other hand, for symmetrical super-capacitors C_{tot} is limited to 0.25 C_{AC} because the relevant formula is: $1/(m_{tot}C_{tot}) = 2/(m_{AC}C_{AC})$, with m_{tot} being $2m_{AC}$ in this case.

Conducting polymers and metal oxides that utilize redox reactions have been suggested as the asymmetric counterpart for AC electrodes in hybrid super-capacitors.[1,2] To further increase the specific capacity, both the positive (e.g. $LiMn_2O_4$) and negative (e.g. graphite, $Li_4Ti_5O_{12}$) intercalation electrodes of lithium-ion batteries (LIB) have been utilized, while graphite (i.e. Li_xC_6) seems to have the most widespread and practical usage.[3–7] The introduction of LIB electrodes to hybrid capacitors gave rise to two major complications: 1) sluggish insertion reactions (i.e. the rate is lower by at least an order of magnitude compared to other hybrid capacitors) and 2) the need for Li^+ pre-intercalation of graphite, what significantly complicates elaborating hybrid capacitors with Li-graphite negative electrodes. An effective solution has been made by nano-sizing lithium titanate ($Li_4Ti_5O_{12}$) on carbon nanofiber with up to 70% of active material mass loading, which leads to high rate and stable cycle performances.[5,7]

Magnesium is a unique active metal for negative electrodes for batteries, with a volumetric capacity of 3833 mAh cc^{-1} that far exceeds that of lithium (2046 mAh cc^{-1}). Moreover Mg deposition, when the right solutions are used (to be discussed later), does not form dendrites, which is the major issue regarding the use of lithium metal anodes in rechargeable batteries.[8,9] Owing to its great abundance in the earth's crust (the 8th most abundant element), Mg can serve as an active element for sustainable energy storage.[10] Because the passivation films formed on Mg anodes are not permeable to Mg^{2+} ions, reversible Mg deposition/dissolution requires special kinds of solutions based on ether solvents and Mg organo-haloaluminate complex electrolytes that does not form passivation films on Mg electrodes.[11] Matching these complex electrolyte solutions with positive electrodes is extremely challenging because of compatibility issues; the Mg organo-haloaluminate electrolytes are often nucleophilic and chemically reactive toward electrophilic oxide electrodes. Furthermore, the large ionic size of the Mg ionic complexes limits the usage of porous carbon positive electrodes in the Mg organo-haloaluminate electrolytes.

This paper focuses on the ionic size issue, aiming to develop a prototype of Mg hybrid capacitor (MHC) cells. Previous studies have revealed that LiCl or tetraalkylammonium-chloride can be dissolved in the ethereal Mg organo-haloaluminate complex solutions, enhancing the kinetics and efficiency of Mg deposition/dissolution processes.[12] We adopted this strategy to modify selected ethereal complex electrolyte solutions by introducing smaller ionic species to the solution. We elaborated MHC cells comprising monolithic AC cloth capacitive positive electrodes, Mg foil negative electrodes and modified ethereal-Mg organo-haloaluminate complex electrolyte solutions. The cells developed in this work exhibited up to 90 F g^{-1} of AC's specific capacitance within a 0.5–2.4 V potential range (vs. Mg^{2+}/Mg) with a stable cycle performance (>4000 cycles measured).

Experimental

Material preparations.— ACC-5092-20 (Kynol, BET surface area = 2000 m^2 g^{-1}) activated carbon cloth was used as the positive electrode, after drying it under vacuum at 120°C overnight. The overall pore diameter is less than 2 nm (from nitrogen gas adsorption measurements and related pore size distribution using the DFT model).[13] The Mg foil negative electrodes were scratched by a slide glass until fresh surface was exposed just before introducing it to glove box. 3 V class Mg complex electrolyte solutions were synthesized as follows:[14] **1)** predetermined amount of aluminum chloride ($AlCl_3$) powder was added very slowly (slow enough to avoid the continuous evolution of a white fog) into THF under vigorous stirring, followed by an overnight stirring. **2)** The $AlCl_3$/THF solution was added slowly into a pre determined amount of 2 M phenyl-magnesium-chloride (PhMgCl)/THF solution under vigorous stirring, followed by an overnight stirring. The precursors for the synthesis of Mg complex electrolyte solutions, 2 M PhMgCl/THF solution, $AlCl_3$ anhydrous powder (99.999%), and THF (anhydrous, >99.9%), were purchased from Aldrich. From previous studies[14] we know that this synthesis involves trans-metalation reactions in which all the organic ligands are bonded with the Al cations while Mg cations are bound to chloride moieties and are stabilized by THF solutions. The solutions thus prepared contained 0.25 M

*Electrochemical Society Active Member.
**Electrochemical Society Fellow.
zE-mail: Doron.Aurbach@biu.ac.il

of $Mg_2Cl_3^+$ cations and $AlPh_2Cl_2^-$ anions in THF (solvent molecules are involved as coordinating agents that stabilize these ions). These solutions were further modified by adding to them 0.5 M lithium chloride (LiCl) with stirring during 6 hours. Ionic conductivity was measured by Metrohm 644 conductometer and conductivity measuring cell (6.0908.110, cell constant = 0.8 cm^{-1}).

Electrochemical characterizations.— 3-electrode flooded cells were prepared using the three components: AC cloth (1.5 cm^2 size, ca. 21 mg, positive electrode), Mg foils (3 cm^2 size for a negative electrode and a strip for a reference electrode), and the above described complex electrolyte solutions. A platinum wire served as the current collector for the AC cloth. To minimize the Ohmic resistance, the AC cloth and the Mg foil were sandwiched using glass fiber paper (Pall, 300 μm thick) as the separator with applying light compression. Cyclic voltammetry (CV), electrochemical impedance, and galvanostatic charge-discharge tests were carried out in 0.5–2.5 V range vs. Mg^{2+}/Mg (VMP-2 potentiostat, Biologic). The cells were operated in a heating bath that ensures a constant temperature of 30°C. Electrochemical impedance was measured by applying 5 mV rms amplitude in the frequency range of 1 mHz–200 kHz. For rate capability tests, the discharge (or, charge) current was varied from 0.1 to 20 mA after the full charge (or, discharge). A full charge/discharge cycle was ascertained by a constant current step ($|I| = 1$ mA) followed by a constant potential step until $|I| < 0.1$ mA. For cycleability tests, two operational modes were applied: 1) slower (2 mA) and shallower (1.2–2.2 V vs. Mg^{2+}/Mg) charge-discharge and 2) faster (5 mA) and deeper (0.9–2.4 V vs. Mg^{2+}/Mg) charge-discharge. The cell rested for 10 s before and after each step to check the open circuit potential.

Results and Discussion

Fundamental studies on the electrolyte solutions and the AC electrodes.— The 0.25 M Mg organo-haloaluminate complex electrolyte (in THF) solution, and the 0.25 M complex solution containing 0.5 M LiCl, were initially analyzed by cyclic voltammetry with Pt electrodes (Fig. 1). Mg is reversibly deposited and dissolved in these solutions. While similar voltage windows were obtained with both solutions, the LiCl containing solution shows a better Mg deposition/dissolution performance in terms of lower over-potential for Mg deposition. Similar phenomenon has been observed upon the addition of LiCl in another Mg complex electrolyte, 0.25 M $Mg(AlCl_2BuEt)_2$ in THF.[12]

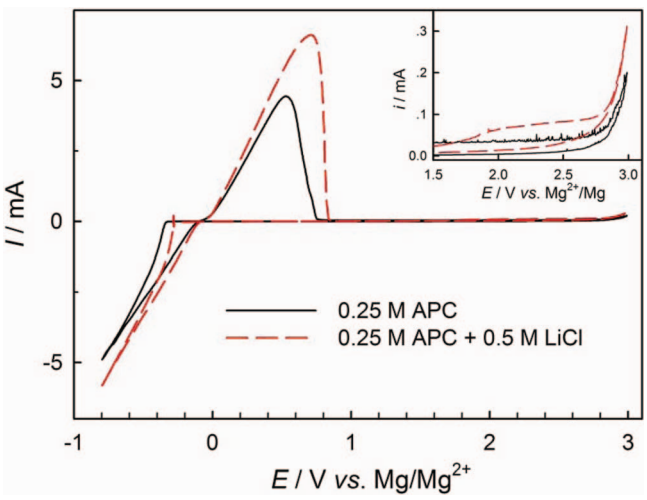

Figure 1. (Color online) Cyclic voltammograms of Pt electrode in solution comprising THF and 0.25 M $Mg_2Cl_3^+$ - $AlPh_2Cl_2^-$ complex electrolyte (denoted as APC – all phenyl complex solution) and in THF solution containing the same complex electrolyte + 0.5 M LiCl (scan rate = 25 mV s^{-1}).

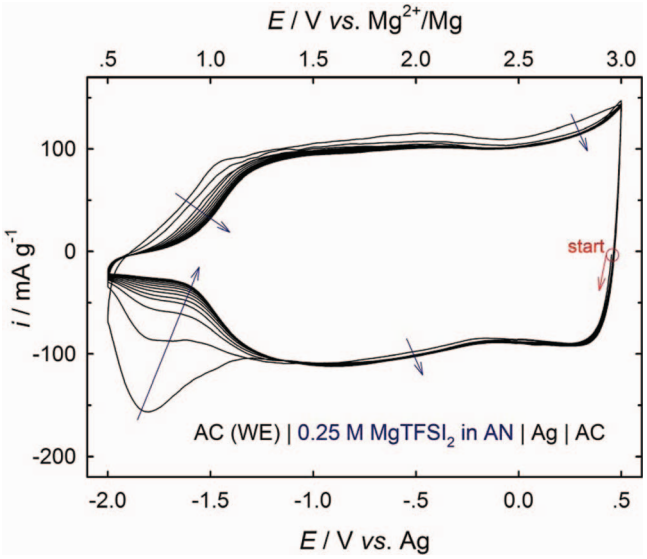

Figure 2. (Color online) Cyclic voltammogram of the AC cloth electrode in 0.25 M $MgTFSI_2$ in acetonitrile (AN) with respect to Ag quasi-reference electrode (scan rate = 1 mV s^{-1}).

Also, the random current spikes usually seen in the voltammograms of Pt electrodes in these complex solutions, attributed to a break-and-repair mechanism of specifically adsorbed anionic species on the Pt surface,[15] are mitigated with the LiCl containing solution (inset of Fig. 1). A suitable electrolyte solution for porous electrodes must be absolutely stable at the operational potentials. Faradaic side reactions if exist even to a minor extent are amplified by the high surface area. In order to ensure the lack of side reactions in these systems, the operational potential of the porous carbon electrodes was limited to <2.5 V vs. Mg^{2+}/Mg, considering the anodic stability window of the solutions used herein (inset of Fig. 1).

The AC electrode's electrochemical properties were also studied in a 'conventional' organic electrolyte solution containing a 'simple' inorganic Mg salt namely 0.25 M magnesium(II) bis(trifluoromethanesulfonyl)imide ($MgTFSI_2$) in acetonitrile (AN). Cyclic voltammetry was performed between 0.5 V to –2.0 V vs. a Ag quasi-reference electrode (the open circuit potential of an Ag wire electrode in this solution is ca. 2.5 V vs. Mg^{2+}/Mg),[16] while the potential sweep started at 0.5 V vs. Ag toward the negative direction (Fig. 2). Typical rectangular shape cyclic voltammograms are obtained in the range of –1.25 to 0.5 V vs. Ag (reflecting a purely capacitive behavior), with ca. 100 F g^{-1} of specific capacitance. The potential of zero charge (pzc) was measured to be around –0.1 V vs. Ag (2.4 V vs. Mg^{2+}/Mg) from the local minimum of the cyclic voltammograms. At $E <$ pzc, cations are adsorbed on the carbon surface and into its pores. The triangular shape of the voltammograms at the lower potentials (< –1.3 V) reflects a sieving behavior of the carbon electrodes toward solvated magnesium ions that cannot enter into too small pores. Hence, this knob-shaped cyclic voltammogram of the porous carbon electrode in this solution is attributed to the saturation of pores with ions before reaching the potential limit.[17] Even if the AC electrode would work well at lower potentials, Mg metal electrodes do not work in this electrolyte solution due to the instant formation of passivation films that block them and avoid any possible Mg ions transport.[16]

The electrochemical behavior of the AC electrode in the complex electrolyte solutions.— After the preparatory analyses, the AC cloth electrodes were studied in the complex electrolyte solutions (Fig. 3). Their pzc value was ca. 2.3 V vs. Mg^{2+}/Mg, which agrees with the value measured in 0.25 M $MgTFSI_2$/AN solution. For the solution without LiCl the adsorption/desorption currents start to diminish at 2.0 V vs. Mg^{2+}/Mg, and the knob-shape (i.e. the sieving effect) is clearly seen at potentials below 1.5 V vs. Mg^{2+}/Mg (solid line of

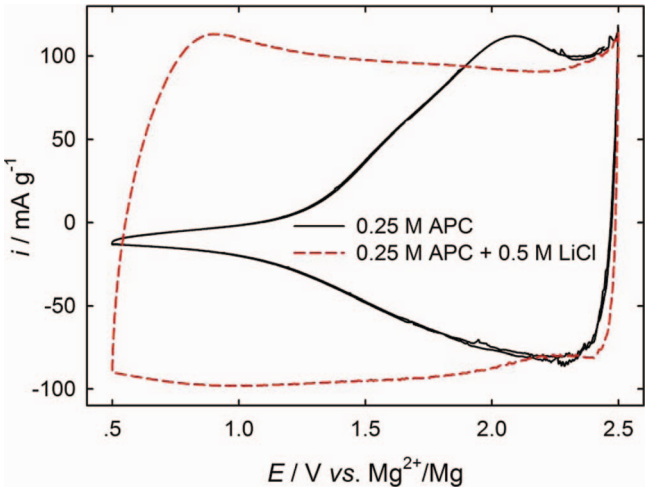

Figure 3. (Color online) Typical cyclic voltammograms of AC cloth electrode in 0.25 M APC solution with or without 0.5 M LiCl (scan rate = 0.1 mV s^{-1}).

Fig. 3). In comparison with the cyclic voltammogram in AN electrolyte, the 'saturation of the pores' appears at much higher potentials (by 1 V) in the complex electrolyte solution. This can be attributed to the larger ionic size of the Mg complex ions compared to that of Mg ions in conventional electrolyte solutions. Therefore this problem can be overcome either by increasing the pore size or by decreasing the ions' size. In the modified complex electrolyte solutions that contain Li^+ and Cl^- (relatively small) ions the cyclic voltammograms of the AC electrodes exhibit a rectangular, capacitive shape in the potential range 2.5–0.5 V vs. Mg^{2+}/Mg (dashed line in Fig. 3).

The specific capacitance is ca. 90 F g^{-1}, which is close to the specific capacitance that can be obtained with the same AC electrode in the tetra-alkyl ammonium salt solutions in AN or propylene carbonate (PC) that are used in non-aqueous super-capacitors (100–120 F g^{-1}).[18] In addition, the AC electrode's impedance in the LiCl free complex electrolyte solution is 3 times larger than that in the LiCl containing solution both at highest and lowest frequency limits (Fig. 4). This effect of the presence of LiCl in solutions is attributed to

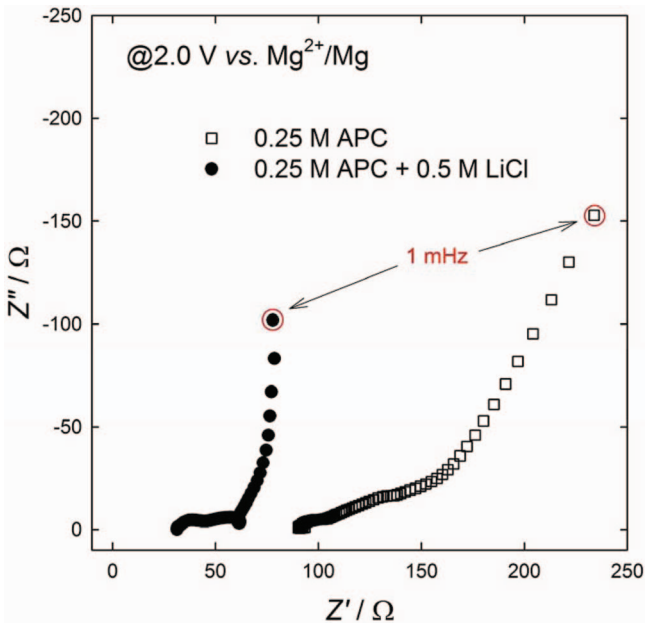

Figure 4. (Color online) Impedance profiles of AC cloth electrode at 2.0 V vs. Mg^{2+}/Mg in solutions comprising THF and 0.25 M $Mg_2Cl_3^+$ - $AlPh_2Cl_2^-$ complex electrolyte (APC solution) with or without 0.5 M LiCl.

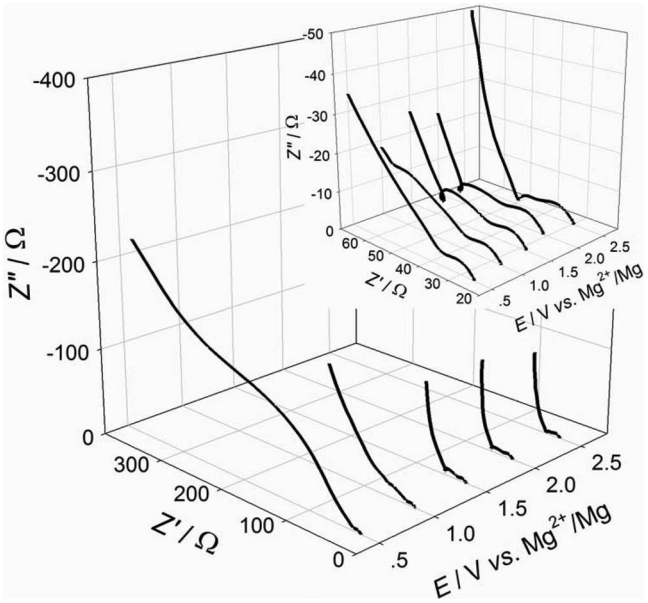

Figure 5. (Color online) EIS spectra of AC cloth electrode in solution comprising THF and 0.25 M $Mg_2Cl_3^+$ - $AlPh_2Cl_2^-$ complex electrolyte (APC solution) + 0.5 M LiCl.

a smaller diffusional resistance in the pores for Li and Cl ions (in the low frequency region) as well as to a lower bulk solution resistance (at the highest frequency). The ionic conductivity values of 0.25 M APC with and without 0.5 M LiCl were measured as 2.7 and 2.1 mS cm^{-1}, respectively. It is noteworthy that LiCl is strongly associated in THF and the conductivity of the 0.5 M LiCl in THF solution is negligible ($<10^{-2}$ mS cm^{-1}). Therefore, the increase in the ionic conductivity by the addition of LiCl can be explained by a reaction of LiCl with Mg complex electrolyte, which results in dissociated Li ionic species.[12] Throughout this comparative analysis, LiCl added Mg complex electrolyte solution was chosen to construct and demonstrate Mg hybrid capacitors.

The adsorption/desorption kinetics of AC cloth electrodes in the LiCl containing solutions were studied by electrochemical impedance spectroscopy (EIS) as a function of the electrodes' potential. It was found that the impedance begins to increase at <1 V vs. Mg^{2+}/Mg and is extremely large at 0.5 V vs. Mg^{2+}/Mg. this can be attributed to the hindrance for further ions transport by the already adsorbed ions in the pores (Fig. 5). Even if the pores are not saturated, kinetic issues still persist due to hindrance and repulsion among co-ions. The large impedance at 0.5–1.0 V vs. Mg^{2+}/Mg implies that the energy-efficiency and the mechanical stability of the electrodes may be poor at too low potentials. Therefore the operational potential should be $E > 0.5$ V vs. Mg^{2+}/Mg in order to maximize energy-efficiency and cycling stability.

Operation of AC cathode |LiCl added Mg complex ethereal solution |Mg anode full-cell.— Fig. 6 shows discharging and charging rate capabilities of a prototype full cell of Mg hybrid capacitor (i.e., using Mg metal anode and activated carbon cathode). The voltage profiles of the positive and the negative electrodes were simultaneously measured using an Mg reference electrode. Each pair of voltage profiles were measured upon varied discharge/charge current after a full charge/discharge, respectively. The charge and discharge cutoff potentials used were 2.4 and 0.9 V vs. Mg^{2+}/Mg, respectively (black lines in Fig. 6). I = 0.1 mA and 20 mA corresponded to 6 h and 2 min charge (or discharge), respectively. At $I < 0.5$ mA, the capacitance of the positive electrode reaches 90 F g^{-1} (or, 37.5 mAh g^{-1} of capacity for the operational potential range) and the voltage drop is negligible. At higher currents, a voltage drop at the beginning of the charge/discharge (*IR*-drop) is observed (up to 0.2 V drop at

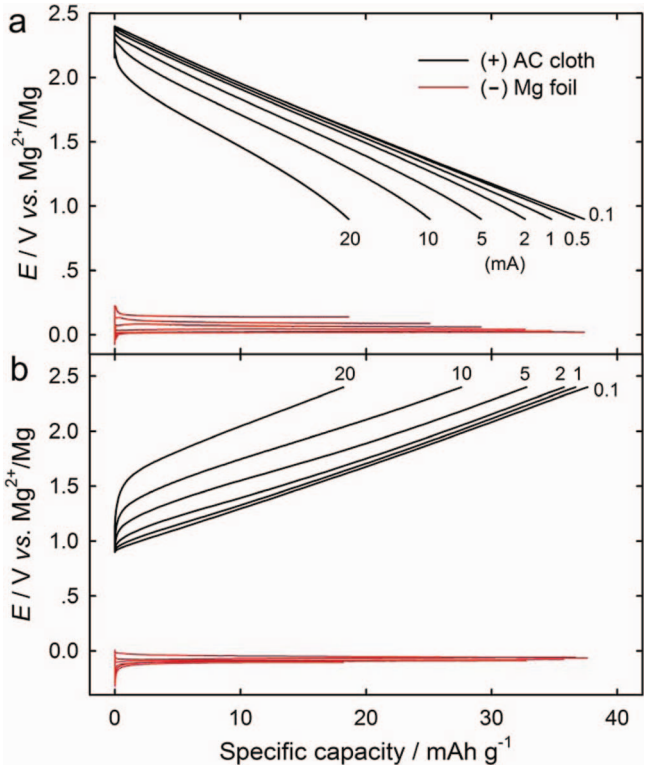

Figure 6. (Color online) Rate capabilities of AC cloth (+) | complex THF solution (denoted as APC) + 0.5 M LiCl | Mg (RE) | Mg (–) cell upon (a) discharge and (b) charge after full charge and discharge, respectively.

20 mA) along with a significant drop in utilizable capacitance (down to 52 F g^{-1} at 20 mA, calculated from the slope). This means that two parameters are individually affected by the charging/discharging current: *IR*-drop and utilizable capacitance. The *IR*-drop depends on the internal resistance of the cell (mainly ionic resistance of the electrolyte solution) while the utilizable capacitance is determined by the kinetics of the ionic movement through the pores.

Even though the potential profiles of the positive electrode is influenced significantly by the charge/discharge currents, the potential profiles of the Mg foil negative electrodes (red lines of Fig. 6) is virtually constant, and close to 0 V vs. Mg^{2+}/Mg regardless of the current density used. There are some potential spikes at the beginning of the charge/discharge process, but they stabilize later to a constant value of <0.2 V and <0.1 V for Mg dissolution and deposition, respectively, depending on the current magnitude. This finding suggests that the kinetics of Mg deposition/dissolution is fast enough to be matched with AC electrodes.

The cycling performance was studied by two different operational modes: shallower/slower mode and deeper/faster mode.

Shallower/slower mode.—The hybrid Mg/AC cells were cycled at 2 mA within the range of 1.2–2.2 V (Fig. 7). The capacitance retention was 93% by the 2270th cycle and the coulombic efficiency was ~100%. The linearity of the voltage profile is well-reserved in this operational mode (in the inset of Fig. 7). The potential of the Mg electrode was virtually constant, at ~10 mV.

Deeper/faster mode.—The hybrid Mg/AC cells were cycled at 5 mA within the range of 0.9–2.4 V (Fig. 8). The capacitance retention was 79% by the 4500th cycle and the coulombic efficiency was ~100%. The capacitance retention profile fluctuates periodically, mainly due to the daily and weekly temperature variances (30~35°C); generally, the higher the temperature, the higher is the capacitance. It is noteworthy to mention that the fluctuation due to temperature was not so significant at the shallower/slower mode, even though the relevant cells were in a same bath. Ionic mobility is kinetically more demanding at deeper/faster operation of AC electrodes, so that the capacitance is more sensitive toward temperature fluctuations. Upon discharging the AC electrodes, the slope becomes steeper at potentials <1.5 V vs. Mg^{2+}/Mg (in the inset of Fig. 8). This finding supports the kinetic hindrance at potentials <1.5 V vs. Mg^{2+}/Mg that was observed in the EIS measurements. The over-potential of Mg dissolution/deposition was ~50 mV. The specific capacitances in Figs. 7 and 8 were calculated without *IR*-correction. If they are *IR*-corrected (i.e., only the slope is considered for capacitance calculation), the specific capacitance values are ca. 80 F g^{-1}.

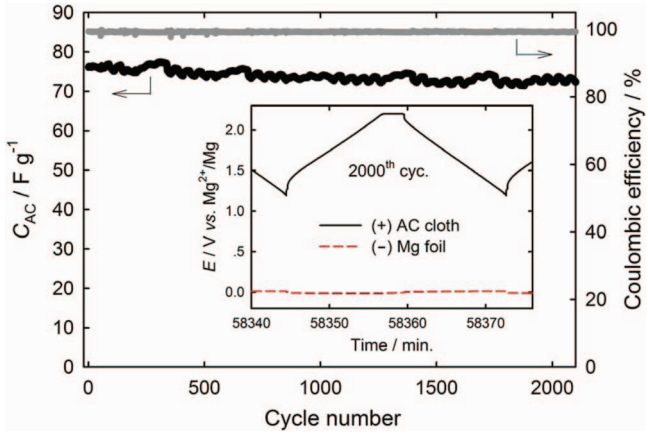

Figure 7. (Color online) Cycling performance of AC cloth (+) | 0.25 M APC solution + 0.5 M LiCl electrolyte | Mg (RE) | Mg (–) cell. Operating potential range was from 1.2 V to 2.2 V vs. Mg^{2+}/Mg. Charge-discharge current was 2 mA. Constant voltage was maintained at 2.2 V vs. Mg^{2+}/Mg until I < 0.2 mA.

Since the electric double layer charging is a physical process, it is generally not affected by temperature. And the observed temperature dependency can be explained by either 1) the increase in the ionic conductivity of the electrolyte or 2) the facilitation of ionic diffusion into the micropores at increased temperature. First possibility was discarded since the *IR*-drop is almost constant regardless of the temperature (0.15 V at 5 mA and 0.05 V at 2 mA). It means that the ionic conductivity of the bulk electrolyte is not so sensitively affected by the temperature. Rather, the slope at <1.2 V vs. Mg^{2+}/Mg is sensitively changed by temperature, which is in accordance with the larger impedance at <1.5 V vs. Mg^{2+}/Mg (Fig. 5). Therefore, our best answer for "the reason why the specific capacitance is dependent on the temperature" will be an Arrhenius type behavior of ionic species' diffusion into the micropores at the low potential region, where significant kinetic barrier is involved by the already adsorbed large

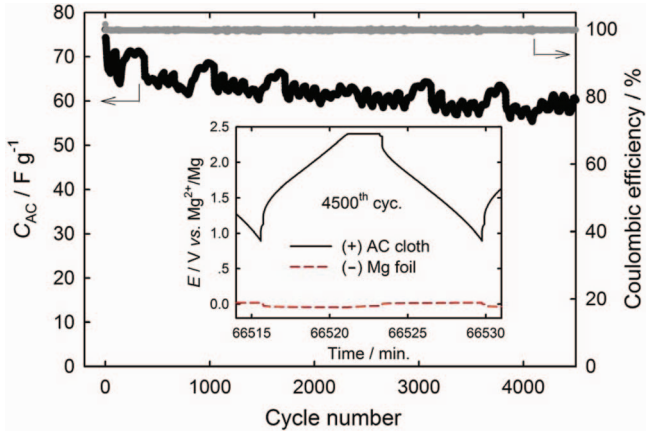

Figure 8. (Color online) Cycling performance of AC cloth (+) | 0.25 M APC solution + 0.5 M LiCl electrolyte | Mg (RE) | Mg (–) cell. Operating potential range was from 0.9 V to 2.4 V vs. Mg^{2+}/Mg. Charge-discharge current was 5 mA. Constant voltage was maintained at 2.4 V vs. Mg^{2+}/Mg until I < 1 mA.

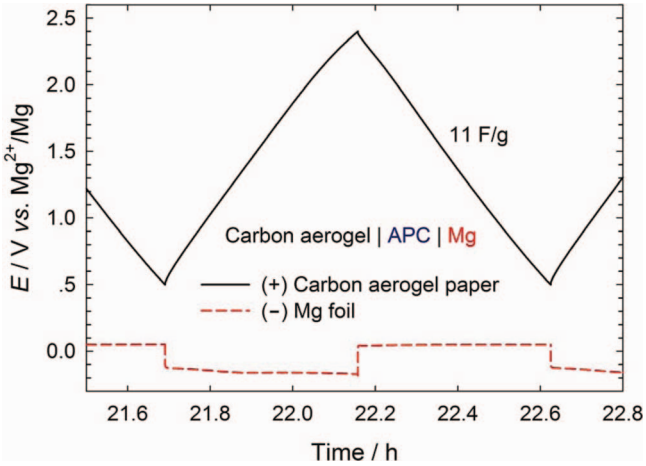

Figure 9. (Color online) Voltage profiles of carbon aerogel paper (+) | 0.25 M APC solution | Mg (RE) | Mg (–) cell ($I = 0.1$ mA). Carbon aerogel paper was provided by READE (BET surface area = 450 m^2 g^{-1} and pore diameter = 20–40 nm).

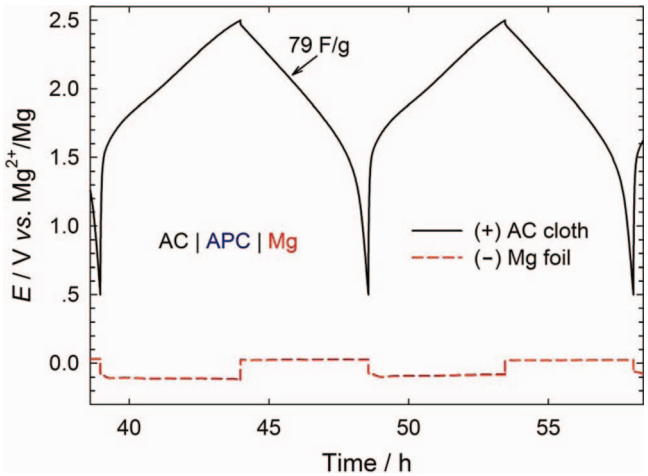

Figure 10. (Color online) Voltage profiles of AC cloth (+) | 0.25 M APC solution| Mg foil (–) full-cell.

ionic species that sterically hinder further ionic diffusion into the pores.

Considerations for further applications: potential use for discovery of the active ions' size and identity.— Fundamentally, porous carbon electrodes with controlled pore size can be used to measure the average ionic size of Mg complex electrolytes. Until now, the identification of the active ions in the Mg complex electrolytes has been controversial; some scholars believe that only $Mg_2Cl_3 \cdot 6THF^+$ corresponds to the Mg deposition/dissolution while others consider also $MgCl \cdot 5THF^+$ cations to be relevant for non-aqueous Mg electrochemistry. Determination of Mg ionic size by porous carbon electrodes with well-defined pore size can shed light on the molecular structure of the active ions, complementarily with ionic conductivity measurement.

Considerations for mass production of Mg hybrid capacitors.— In the Mg hybrid capacitors, the Mg ionic species move in a "shuttlecock" mode similar to batteries, while Li ions in the electrolyte solutions are "consumed-recovered" (adsorbed/desorbed), in a capacitive mode as is typical for EDLC. Thus, during discharge of these cells Mg and Li ions are introduced into the pores of the AC positive electrode while Mg ions are produced on the surface of the Mg negative electrode (due to Mg dissolution). During charge, Mg and Li ions are desorbed from the pores of AC positive electrodes while Mg ions reduced on the surface of Mg negative electrode to Mg metallic deposits. Therefore, the total equivalents of Mg and Li ions is conserved, while the individual concentrations of Li and Mg ions fluctuate during the periodic charge-discharge processes. In order to prevent Li ions starvation during charge-discharge of the AC cloth electrode (15 mg/cm^2), the electrolyte solution layer thickness should be 300–460 μm, which can be covered by the free volume of AC cloth and separator considering their usual practical thickness values (550 μm and 300 μm, respectively). In the Mg negative electrode side, chemical/electrochemical pretreatment may be important for long term operation of Mg metal electrodes in such devices.[19]

Future works.— The pore structure of the AC cloth electrode used herein was not optimized for ideal and most effective EDLC application. The aim of this work is to demonstrate the Mg-AC hybrid capacitor concept. Higher rate capability and specific capacitance can be attained by developing meso-porous carbon electrodes. Ideally, it would be preferable if there will be no need to include in the solutions Li ions, by introducing such mesoporous electrodes. For a preliminary example, electrodes comprising meso-porous carbon aerogel (READE, S_{BET} = 450 cm^2 g^{-1}, pore diameter = 20–40 nm) showed a straight voltage profile down to 0.5 V vs. Mg^{2+}/Mg even in complex ethereal electrolyte solution that does not contain Li ions at all (Fig. 9, compare it with the response of the AC cloth electrode presented in Fig. 10). The capacitance of the aerogel carbon electrode was relatively low, due to the limited total specific surface area (450 m^2/g for this carbon, compared to 2000 m^2/g for the AC used herein as the main positive electrode); however, the shape of the voltage profile demonstrates the better kinetics of adsorption/desorption of the relatively big ions into the meso-porous carbon electrode. Introduction of alternative chloride salts other than LiCl is also of interest to realize non-lithium system. The solubility of NaCl was extremely low in the Mg complex electrolyte; however, tetraalkylammonium chloride may be an effective alternative, as it has been known to modify Mg complex electrolyte in a similar way with LiCl.[12] Finally, fundamental innovation can be made by developing Mg electrolyte systems with smaller ions size and wider voltage window for high energy and power densities.

Conclusions

The concept of Mg hybrid capacitor (MHC) was successfully demonstrated for the first time. Powered by a low potential, large capacity, and the non-dendritic morphology of a preferential Mg metal negative electrode, MHC can provide higher energy and power densities compared with other hybrid capacitors. The performance of these systems could be enhanced significantly by introducing Li ions of small ion size into the Mg complex ethereal electrolyte solution, so that higher specific capacitance (90 F g^{-1}) and wider operational voltage (0.5–2.4 V) was attained together with kinetic benefits for both the AC and the Mg electrodes. Thus assembled cells comprising AC cloth (+) cathodes, Mg foil (–) anode and electrolyte solution comprising THF (solvent) and $Mg_2Cl_3^+$, $AlPh_2Cl_2^-$, Cl^- and Li^+ ions operated for >4500 cycles with stable cycling performance and 100% coulombic efficiency. The ionic size or pore size control is the key for the further development of more advanced MHC systems.

Acknowledgment

This research was supported by Pellion Technologies and ARPA-E award DE-AR0000062 and the BSF, Israel-US bi-national science foundation.

References

1. A. Laforgue, P. Simon, J. F. Fauvarque, M. Mastragostino, F. Soavi, J. F. Sarrau, P. Lailler, M. Conte, E. Rossi, and S. Saguatti, *J. Electrochem. Soc.*, **150**, A645 (2003).

2. V. Khomenko, E. Raymundo-Piñero, E. Frackowiak, and F. Béguin, *Appl. Phys. A*, **82**, 567 (2006).
3. A. Du Pasquier, I. Plitz, S. Menocal, and G. Amatucci, *J. Power Sources*, **115**, 171 (2003).
4. Y.-g. Wang and Y.-y. Xia, *Electrochem. Commun.*, **7**, 1138 (2005).
5. K. Naoi, *Fuel Cells*, **10**, 825 (2010).
6. D. Cericola, P. Novák, A. Wokaun, and R. Kötz, *J. Power Sources*, **196**, 10305 (2011).
7. K. Naoi, S. Ishimoto, J.-i. Miyamoto, and W. Naoi, *Energy Environ. Sci.*, **5**, 9363 (2012).
8. M. Matsui, *J. Power Sources*, **196**, 7048 (2011).
9. C. Ling, D. Banerjee, and M. Matsui, *Electrochim. Acta*, **76**, 270 (2012).
10. H. D. Yoo, I. Shterenberg, Y. Gofer, G. Gershinsky, N. Pour, and D. Aurbach, *Energy Environ. Sci.*, **6**, 2265 (2013).
11. D. Aurbach, in *Nonaqueous Electrochemistry*, D. Aurbach Editor, p. 289, Marcel Dekker, New York (1999).
12. Y. Gofer, O. Chusid, H. Gizbar, Y. Viestfrid, H. E. Gottlieb, V. Marks, and D. Aurbach, *Electrochem. Solid-State Lett.*, **9**, A257 (2006).
13. R. Elazari, G. Salitra, A. Garsuch, A. Panchenko, and D. Aurbach, *Adv. Mater.*, **23**, 5641 (2011).
14. O. Mizrahi, N. Amir, E. Pollak, O. Chusid, V. Marks, H. Gottlieb, L. Larush, E. Zinigrad, and D. Aurbach, *J. Electrochem. Soc.*, **155**, A103 (2008).
15. N. Pour, Y. Gofer, D. T. Major, and D. Aurbach, *J. Am. Chem. Soc.*, **133**, 6270 (2011).
16. Z. Lu, A. Schechter, M. Moshkovich, and D. Aurbach, *J. Electroanal. Chem.*, **466**, 203 (1999).
17. R. Mysyk, E. Raymundo-Pinero, and F. Beguin, *Electrochem. Commun.*, **11**, 554 (2009).
18. N. Handa, T. Sugimoto, M. Yamagata, M. Kikuta, M. Kono, and M. Ishikawa, *J. Power Sources*, **185**, 1585 (2008).
19. Y. Gofer, O. Chusid, and D. Aurbach, in *Encyclopedia of Electrochemical Power Sources*, G. Jürgen Editor, p. 285, Elsevier, Amsterdam (2009).